Vol. 14, pp. 111–117 (2017)
doi: 10.2142/biophysico.14.0_111

Biophysics and Physicobiology
https://www.jstage.jst.go.jp/browse/biophysico/

Regular Article

Demonstration of correlative atomic force and transmission electron microscopy using actin cytoskeleton

Yutaro Yamada[1,3], Hiroki Konno[2] and Katsuya Shimabukuro[1]

[1]*Department of Chemical and Biological Engineering, National College of Technology, Ube College, Ube, Yamaguchi 755-8555, Japan*
[2]*Bio-AFM Frontier Research Center, Kanazawa University, Kanazawa, Ishikawa 920-1192, Japan*
[3]*Present address: Graduate School of Natural Science & Technology, Kanazawa University, Kanazawa 920-1192, Japan*

Received December 14, 2016; accepted June 29, 2017

In this study, we present a new technique called correlative atomic force and transmission electron microscopy (correlative AFM/TEM) in which a targeted region of a sample can be observed under AFM and TEM. The ultimate goal of developing this new technique is to provide a technical platform to expand the fields of AFM application to complex biological systems such as cell extracts. Recent advances in the time resolution of AFM have enabled detailed observation of the dynamic nature of biomolecules. However, specifying molecular species, by AFM alone, remains a challenge. Here, we demonstrate correlative AFM/TEM, using actin filaments as a test sample, and further show that immuno-electron microscopy (immuno-EM), to specify molecules, can be integrated into this technique. Therefore, it is now possible to specify molecules, captured under AFM, by subsequent observation using immuno-EM. In conclusion, correlative AFM/TEM can be a versatile method to investigate complex biological systems at the molecular level.

Corresponding authors: Hiroki Konno, Bio-AFM Frontier Research Center, Kanazawa University, Kakuma-machi, Kanazawa, Ishikawa 920-1192, Japan. e-mail: hkonno@se.kanazawa-u.ac.jp; Katsuya Shimabukuro, Department of Chemical and Biological Engineering, National College of Technology, Ube College, 2-14-1 Tokiwadai, Ube, Yamaguchi 755-8555, Japan. e-mail: kshimabu@ube-k.ac.jp

Key words: correlative microscopy, immune electron microscopy, patterned substratum

Atomic force microscopy (AFM) is a powerful technique for investigating the structures of dry and wet biological specimens at nanometer spatial resolution [1,2]. Despite its capacity for generating fine topological images, applying AFM in biological sciences has been mostly limited to simple systems in which only one or a few types of biomolecules exist [3–5]. This is primarily because AFM cannot be used to specify molecules [6]; therefore, its use should be complimented by other methods to broaden the applications of AFM to complicated biological systems.

Correlative microscopy can be a potential solution for expanding the applications of AFM [7]. Combining AFM with fluorescence microscopy (FM) is the first choice, and thus, has been developed by several groups [8–14]. FM is designed to observe the location and dynamics of a target molecule, tagged with a fluorescence marker, at the video rate of 30 frames per second, making it suitable for complementing AFM. In recent studies, Fukuda *et al.* have combined AFM with total internal reflection fluorescence microscopy (TIRF) to monitor the movement of a single molecule using AFM and TIRF simultaneously [12]. AFM has also

◀ ***Significance*** ▶

We report a new microscopy technique called correlative atomic force and transmission electron microscopy (correlative AFM/TEM) in which a targeted region of a sample can be observed under both AFM and TEM. Recent advances in AFM have allowed detailed observation of the dynamic nature of biomolecules. However, specifying molecular species by AFM alone still remains a challenge. We demonstrate correlative AFM/TEM using actin filaments, and further show that immune electron microscopy to specify molecules can be integrated into this technique. Thus, correlative AFM/TEM could be a versatile method to investigate complex biological systems at the molecular level.

been combined with super-resolution microscopy, providing a detailed view of the organization of the cytoskeletal filament meshworks using AFM and FM [13,14].

Combining AFM with FM, or other advanced fluorescence techniques, has enabled the application of AFM in complex biological systems. However, these methods remain limited by the disadvantages of fluorescence techniques, such as limited spatial resolution and photo bleaching of conventional fluorescence microscopy and TIRF, and the slow rate of image acquisition of super-resolution microscopy [15,16]. To circumvent these problems, we have developed a method that combines AFM with transmission electron microscopy (TEM). In this study, we describe the design of correlative AFM/TEM and demonstrate correlative AFM/TEM by using actin filaments as a test sample.

Materials and Methods

Reagents

Glutaraldehyde and tannic acid were purchased from Electron Microscopy Sciences (Hatfield, PA); osmium tetroxide from TAAB (Berks, England); and glycine, polyethylene glycol, Tween 20, and $NaBH_4$ from Wako (Osaka, Japan).

Proteins

Actin from rabbit muscle, purified as described in [17], was a kind gift from N. Kodera (Kanazawa University). The actin was polymerized into filaments, stabilized with phalloidin to prevent depolymerization, and stored at 4°C until use. Mouse anti-β-actin antibody and the gold-conjugated secondary antibody were purchased from Sigma (St. Louis, MO). The goat anti-mouse IgG was purchased from BBI (Blaenavon, UK).

Creating a thin layer of patterned gold on coverslips

To prepare cover slips with a thin, patterned layer of gold, a locater grid (style H2; Ted Pella Inc., Redding, CA) was placed on a 24 mm × 40 mm cover slip (Matsunami, Glass Ind., Ltd. Osaka, Japan), and gold was deposited onto the coverslip by evaporation in a vacuum evaporator (SVC-700TMSG; Sanyu Denshi, Tokyo) as described previously [7]. To prevent the gold layer from detaching, the patterned cover slips were baked at 160°C for 12 hours to stabilize the layer. After the coverslips cooled to 25–26°C, the small areas, containing the locater grid pattern, were cut into approximately 2 mm × 2 mm sections using a diamond pen, and then adhered onto the top of a cylindrical glass stage using clear nail polish. The deposited gold possessed a purple color; thus, the pattern was readily visible through an objective lens equipped with AFM. The thin gold layer is electrically dense and, therefore, also visible under TEM [7].

Observation of actin filaments using AFM

Observation of the actin filaments in solution was performed using a laboratory-built high-speed AFM, as described previously [3,5,18,19]. The glass stage, with the patterned cover slips, was mounted, using nail polish, onto a Z piezo element of the AFM scanner. For the observation using AFM, we employed avidin to facilitate effective binding between the glass surface and actin filaments because actin and the glass surface possess negative charges, whereas avidin possesses a positive charge, at pH 7.0. The surface of the coverslip was first coated with 0.05 mg/ml avidin for 10 minutes, then washed four times with 5 µl buffer A (10 mM MOPS, pH 7.0; 0.5 mM $MgCl_2$). Two microliters, containing the actin filaments stabilized with phalloidin, was placed on the stage of the AFM and incubated for 10 minutes at room temperature. After the incubation, the surface was washed twice with buffer A. To provide mechanical strength to the actin filaments, we further chemically fixed the actin filaments with 10 mM MOPS (pH 7.0), 1.25% glutaraldehyde, and 2 mg/ml tannic acid. By monitoring the structure of the actin filaments, using HS-AFM, during the addition of the fixative, we confirmed that the fixation did not alter the morphology of the actin filaments (Supplementary Fig. 1).

After washing with 10 mM MOPS (pH 7.0), imaging was performed using a HS-AFM equipped with small cantilevers (BL-AC10DS-A2 or BL-AC7DS-KU4, Olympus, Tokyo, Japan) and operated in tapping mode. The free oscillation amplitude was ca. 1.5 nm, and the set-point amplitude was 80–90% of the free amplitude. The imaging rate, scan size, and feedback parameters were optimized during the observation to enable visualization with minimal tip force. After the observation, acetone was used to remove the stage of the AFM, with the coverslip, from the AFM scanner without drying out the observed sample. This step was performed carefully, to prevent the acetone from contacting the actin filaments, because it would destroy their structure.

Post-fixation and replica preparation

The coverslip, removed from the AFM stage, was immersed in 10 mM MOPS buffer in a plastic dish and post-fixed using 1% osmium oxide in 30 mM HEPES buffer (pH 7.4) for 1 hour on ice in the dark. After the coverslip was washed five times with distilled water, the specimen was dehydrated using a series of ascending ethanol concentrations from 0 to 100%. The coverslip was then transferred to the chamber in a critical point dryer (CPD2, Hitachi, Tokyo), followed by replacing ethanol with liquid phase CO_2 10 times. Temperature and pressure were raised to the critical point in which liquid phase CO_2 was transformed into the gas phase to minimize surface tension. Platinum/carbon shadowing was performed using a vacuum evaporator, and the replica was recovered under a dissecting microscope.

Transmission electron microscopy and image processing

Specimens were observed under a transmission electron microscope (JEM-2100, JEOL, Tokyo) operated at 80 kV. Images were recorded with a charge-coupled device (CCD)

camera (KeenView, Olympus Soft Imaging Solutions, Tokyo) under the control of a personal computer. Typically, the gold pattern was first located at a low magnification to locate the target region, then returned to a normal magnification mode to observe the actin filaments. Image processing, such as trimming, rotation, and enhancement of contrast, were performed using ImageJ, an image processing program operated using a Windows platform [20].

Results

Choosing the substratum for correlative atomic force and TEM

The outline of our correlative AFM/TEM is summarized in Figure 1. In correlative AFM/TEM, it is necessary to accurately correlate the two images captured separately under different physical conditions. Therefore, a reference marker to facilitate the relocation of the target area in a sample, is important; otherwise, the correlation of the two images is practically impossible. A marker, suitable for this purpose, should generate clear images under AFM and TEM, and should be physically and chemically stable so that it does not impair the function of the biological molecules. To meet these requirements, we chose the method used for correlative light and electron microscopy, in which a pattern of a thin gold layer was deposited on the surface of a coverslip (Fig. 2) [7]. The gold deposit induced a color change on the coverslip from transparent to purple, rendering the reference pattern visible under light microscopy (Fig. 2a–c). Furthermore, the high electron density of the deposited gold prevented the electron beam from penetrating the sample, allowing for the generation of a clear reference image under TEM.

We confirmed that the reference coverslip, prepared using the method described in the Materials and Methods, was clearly visible through an objective lens equipped with the AFM system, when the stage with the reference coverslip

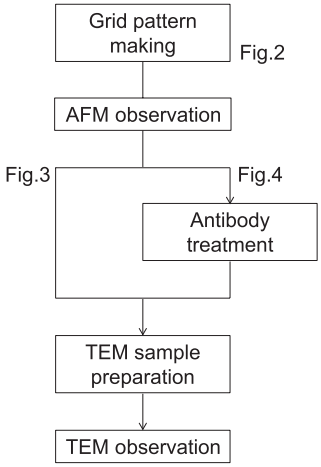

Figure 1 Outline of correlative Atomic Force Microscopy (AFM)/Transmission Electron Microscopy (TEM). Correlative AFM/TEM observation was performed as follows. Actin filaments, immobilized on substratum having a reference pattern, were first observed using AFM, and then using TEM, after TEM specimen preparation. Alternatively, to specifically label the actin filaments with a distinctive marker for TEM, specimens were treated with antibodies before TEM sample preparation.

was set onto the AFM piezoelectric stage; this allowed us to record the position of the cantilever tip relative to the reference pattern (Fig. 2d, e). After observation using AFM, a section of the coverslip was removed from the AFM glass stage and processed to generate a replica as described previously [7]. The electron micrograph of the replica showed a clear image of the reference coverslip obtained using TEM, demonstrating that the reference coverslip can be used as a marker to correlate the images obtained using AFM and TEM (Fig. 2f).

Correlative atomic force and transmission electron microscopy of actin filaments

The actin filaments, stabilized with phalloidin to prevent

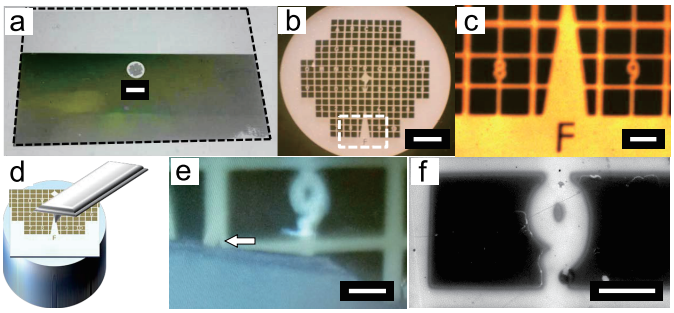

Figure 2 Coverslip, coated with a patterned thin layer of gold, for correlative AFM/TEM. (a) An entire image of a coverslip (24 mm×40 mm) with a gold pattern (3 mm in diameter). (b) A magnified image of the patterned region in the center of the coverslip is shown in (a). (c) A close-up image of the bottom edge of the gold pattern is shown in (b). (d) A schematic drawing of the gold patterned coverslip attached to the flat top of a cylindrical AFM glass stage. The coverslip, trimmed into a small square, was adhered to the AFM glass stage (2 μm×2 μm). A region without gold deposition was scanned by high-speed (HS)-AFM. (e) An image of the patterned coverslip obtained using an objective lens equipped with HS-AFM. The position of the cantilever tip (arrow head), relative to the gold pattern, was monitored. (f) A TEM micrograph of the gold pattern shows a clear view of the pattern under TEM. Scale bar: 3 mm in (a), 500 μm in (b), 100 μm in (c), 50 μm in (e) and (f).

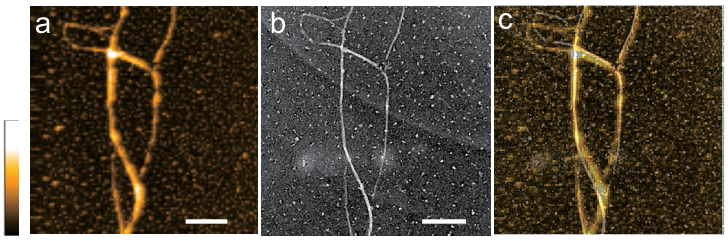

Figure 3 Correlative AFM/TEM observation of actin filaments. (a) An AFM image of actin filaments. Scan rate, 4 s/frame; Z-scale, 61.7 nm. (b) TEM image of the same actin filaments as shown in (a). Scale bar, 500 nm. (c) Superimposed image of (a) and (b).

their disassembly, were immobilized on the avidin-coated surface of a coverslip tagged with the reference marker, and chemically fixed before imaging. As expected, scanning a few square micrometer area of the surface of the coverslip revealed a topological image of several actin filaments. The height of the actin filaments, attached to the avidin-coated surface, was ~13 nm as revealed by observation using AFM (Fig. 3a). By subtracting the height of avidin (~5 nm), the height of an actin filament was estimated to be ~8 nm, which was consistent with the height of actin filaments reported previously [21]. Using the pixel setting of the AFM at 20~30 nm per pixel, we could not identify the typical structural features of the actin filaments, such as the distance of the half-helical pitch (~37 nm) as described [22,23]. However, the characteristic morphological patterns, made by several actin filaments, were useful for identifying a particular area of observation. Immediately after the observation, the coverslip was gently removed from the stage and processed, using a series of preparative procedures, to obtain the replica. Careful investigation of the target area in the replica, using TEM, showed that the very same area used for imaging actin filaments by AFM, was reproduced. The two micrographs, shown in Figure 3a–b, were nearly identical; indicating that the structure of actin filaments was well preserved during the preparation of the replica, though few obvious morphological changes in the actin filaments were found in the superimposed micrographs (Fig. 3c). The morphological changes may result from deformation of specimen during post-fixation and replica preparation. The most likely cause of the deformation is dehydration process in the replica preparation for EM observation. The deformation of specimen might be prevented by carrying out the dehydration process more slowly and carefully. Supplementary Figure 2 shows the result of correlative observation of actin filaments, using AFM/TEM, in another region of interest. The scanning area used for AFM observation, and the size of the cover slips, were 3 μm × 3 μm and 2 mm × 2 mm, respectively. When we used non-grid cover slips, the rate for finding the exact same area under AFM and TEM was estimated to be 0.0002%. However, we could increase the rate up to 30% by using cover slips with a patterned thin layer of gold as a guideline. The decrease in the rate was caused by the detachment of the actin filaments from the specimen during preparation of the replica. In these cases, the areas observed using AFM could not be found using TEM. It is expected that the rate for finding the exact same area will be further increased by optimizing the steps involved in replica preparation.

Integrating immuno-electron microscopy in correlative AFM/TEM to specify a molecule

By integrating immuno-electron microscopy, we can identify molecules in AFM images, which is a major advantage of correlative AFM/TEM. Although AFM can generate precise topological images of the specimen surface, which contains many molecules, it is almost impossible to discern molecular species by AFM alone unless the observed molecules possess unique shapes. To solve this problem, we integrated immuno-electron microscopy (immuno-EM) with our correlative AFM/TEM. Immuno-EM is a powerful method for localizing the targeted biomolecules by using antibodies specific to those biomolecules. Prior to replica preparation, we conducted the correlative AFM/immuno-EM as described above, with several modifications such as quenching the glutaraldehyde-fixed actin filaments, blocking the surface of the substrate with bovine serum albumin (BSA)/polyethylene glycol/Tween 20, and incubating the coverslip with a primary antibody against actin and a secondary antibody conjugated to colloidal gold. For immuno-EM, we found that non-specific binding of the gold-conjugated antibody to the glass surface hampered our ability to specify molecules. Therefore, we screened different blocking conditions to prevent the unwanted binding of the antibody to the substrate. We determined that quenching the sample using glycine, and incubating it with a mixture of BSA and Tween 20, provided the most effective blocking before incubating the sample with the primary antibodies. Under these blocking conditions, the actin filaments, observed using AFM, were specifically labeled with colloidal gold, and limited non-specific binding was detected in the background (Fig. 4). The result of using correlative AFM/immuno-EM to observe the other region of interest is shown in Supplementary Figure 3. To assess the morphological changes in the actin filaments, observed using correlative AFM/immuno-EM, we superimposed the two micrographs in Figure 4a–b (Supplementary Fig. 4) using the same approach as for Figure 3.

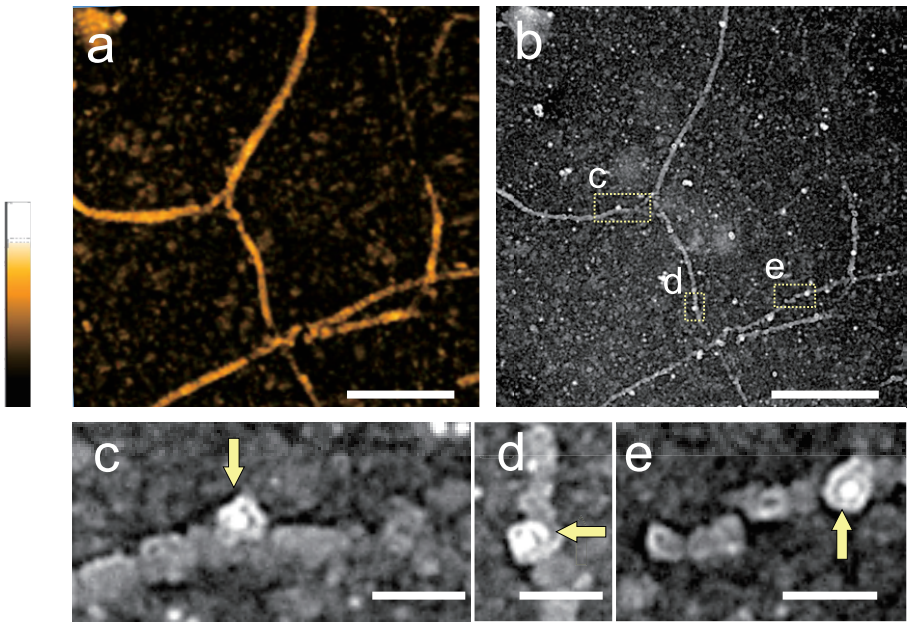

Figure 4 Correlative AFM/immuno-EM of actin filaments. (a) A HS-AFM image of actin filaments. Scan rate, 6 s/frame; Z-scale, 47.8 nm. (b) An immuno-EM image of the same actin filaments as shown in (a). (c–e) Expanded images of the part boxed in (b). Arrows indicate the positions of the gold colloidal particle attached to the actin filaments. Scale bar, 500 nm in (a) and (b), 50 nm in (c)–(e).

Discussion

Rapidly developing microscopy techniques, such as super-resolution and high-speed atomic force microscopy, have overcome the diffraction limit of conventional microscopy and provided significant insight into fundamental biological processes [15,16]. State of the art microscopes can provide useful information, unobtainable a few decades ago. However, every technique has its advantages and limitations. Therefore, when two techniques are integrated to compensate for each other's weaknesses, the combined system can become a more powerful approach to dissecting biological processes at the molecular level. A good example is a combination of correlative atomic force and fluorescent microscopy (correlative AFM/FM) developed by Fukuda *et al*. [12]. The large difference in an area of observation field between FM and AFM affects to correlate their spatial accuracy. The resolution in FM is over 100 times lower than that of AFM, but they improved this difficulty by using wide-area XY scanner. In this technique, a FM module is integrated into an AFM system, thus enabling simultaneous observation of a single molecule under AFM and FM. Using this technique, an investigator can confirm that a targeted molecule, labeled with a fluorescent tag, is truly being observed under AFM. However, to overcome the spatial resolution difference between FM (>200 nm) and HS-AFM (~2 nm) still remains to be improved. Since the spatial resolutions of AFM and EM are very close, correlative AFM/EM has no difficulty for adapting their spatial resolution each other. In addition, unlike FM, both in AFM and EM have no photo bleaching problem of fluorescent dye. By these advantages, correlative AFM/EM method is suitable for observations requiring high spatial resolution and long period of time. Moreover, one drawback of correlative AFM/FM is that a target molecule needs to be labeled with a fluorescent marker, by a chemical or biological method, without impairing the function of the target molecule. Another limitation of correlative AFM/FM is that only one, or a few types, of molecules can be monitored because of the restricted number of fluorophores that can be observed simultaneously under fluorescence microscopy. Conversely, our correlative AFM/TEM does not require any modification of a targeted molecule in advance, making it more versatile than other techniques for correlative microscopy. The one essential requirement for correlative AFM/TEM is an antibody that binds to the targeted molecule specifically. Additionally, optimizing conditions for avoiding the non-specific binding of antibodies to the substrate is requisite for successful correlative AFM/TEM. Numerous studies use AFM to show the interaction between proteins and their antibodies; this can be achieved by simpler procedures, excluding EM, because most of the studies demonstrate a single pair of an antigen and antibody, rather than two or three kinds of pairs simultaneously [24–26]. Immunohistochemical double or triple-labeling methods, which involve changing the size of the gold particle attached to each antibody, are frequently employed for observations using TEM [27–29]. In this study, we showed only the result of a single pairing of actin and its antibody. Employing the double or triple-label immunohistochemical method with TEM is useful for identifying

particular and multiple proteins in heterogeneous systems. Because AFM is used to observe topological structure of a surface, an additional advantage of TEM images is that the gold particle is identified even if it is concealed inside a complicated biological system [30]. In summary, by using actin filaments as a test sample, we have demonstrated that correlative AFM/TEM can be achieved. Therefore, applying this approach to more complicated biological systems is the next challenge.

Acknowledgments

We thank Prof. T. Ando (Kanazawa University) for providing us with experimental instruments. We also thank Assoc. Prof. N. Kodera (Kanazawa University) for fruitful discussion and critical reading of the manuscript. We additionally thank T. Takahashi (Kanazawa University) for conducting part of the AFM observation. This research was supported by Novartis Research Grants (to K. S.); the Center of Innovation Program from Japan Science and Technology Agency, JST (to K. S.); and a Grant-in-Aid for Scientific Research on Innovative Area (No. 25112507 to H. K.) from the Ministry of Education, Culture, Sports, Science, and Technology of Japan.

Conflict of Interest

All authors declare that they have no conflict of interest.

Author Contributions

K. S. and H. K. directed the project and co-wrote the manuscript. Y. Y. performed AFM and TEM experiments and data analysis.

References

[1] Drake, B., Prater, C. B., Weisenhorn, A. L., Gould, S. A., Albrecht, T. R., Quate, C. F., *et al*. Imaging crystals, polymers, and processes in water with the atomic force microscope. *Science* **243**, 1586–1589 (1989).
[2] Bustamante, C., Rivetti, C. & Keller, D. J. Scanning force microscopy under aqueous solutions. *Curr. Opin. Struct. Biol.* **7**, 709–716 (1997).
[3] Kodera, N., Yamamoto, D., Ishikawa, R. & Ando, T. Video imaging of walking myosin V by high-speed atomic force microscopy. *Nature* **468**, 72–76 (2010).
[4] Shibata, M., Yamashita, H., Uchihashi, T., Kandori, H. & Ando, T. High-speed atomic force microscopy shows dynamic molecular processes in photoactivated bacteriorhodopsin. *Nat. Nanotechnol.* **5**, 208–212 (2010).
[5] Uchihashi, T., Iino, R., Ando, T. & Noji, H. High-speed atomic force microscopy reveals rotary catalysis of rotorless F_1-ATPase. *Science* **333**, 755–758 (2011).
[6] Uchihashi, T., Watanabe, H., Fukuda, S., Shibata, M. & Ando, T. Functional extension of high-speed AFM for wider biological applications. *Ultramicroscopy* **160**, 182–196 (2016).
[7] Svitkina, T. M. & Borisy, G. G. Correlative light and electron microscopy of the cytoskeleton of cultured cells. *Meth. Enzymol.* **298**, 570–592 (1998).
[8] Nishida, S., Funabashi, Y. & Ikai, A. Combination of AFM with an objective-type total internal reflection fluorescence microscope (TIRFM) for nanomanipulation of single cells. *Ultramicroscopy* **91**, 269–274 (2002).
[9] Mathur, A. B., Truskey, G. A. & Reichert, W. M. Total internal reflection microscopy and atomic force microscopy (TIRFM-AFM) to study stress transduction mechanisms in endothelial cells. *Crit. Rev. Biomed. Eng.* **28**, 197–202 (2000).
[10] Suzuki, Y., Sakai, N., Yoshida, A., Uekusa, Y., Yagi, A., Imaoka, Y., *et al*. High-speed atomic force microscopy combined with inverted optical microscopy for studying cellular events. *Sci. Rep.* **3**, 2131 (2013).
[11] Gumpp, H., Stahl, S. W., Strackharn, M., Puchner, E. M. & Gaub, H. E. Ultrastable combined atomic force and total internal reflection fluorescence microscope. *Rev. Sci. Instrum.* **80**, 063704 (2009).
[12] Fukuda, S., Uchihashi, T., Iino, R., Okazaki, Y., Yoshida, M., Igarashi, K., *et al*. High-speed atomic force microscope combined with single-molecule fluorescence microscope. *Rev. Sci. Instrum.* **84**, 073706 (2013).
[13] Odermatt, P. D., Shivanandan, A., Deschout, H., Jankele, R., Nievergelt, A. P., Feletti, L., *et al*. High-resolution correlative microscopy: bridging the gap between single molecule localization microscopy and atomic force microscopy. *Nano Lett.* **15**, 4896–4904 (2015).
[14] Chacko, J. V., Zanacchi, F. C., & Diaspro, A. Probing cytoskeletal structures by coupling optical superresolution and AFM techniques for a correlative approach. *Cytoskeleton (Hoboken)* **70**, 729–740 (2013).
[15] Betzig, E., Patterson, G. H., Sougrat, R., Lindwasser, O. W., Olenych, S., Bonifacino, J. S., *et al*. Imaging intracellular fluorescent proteins at nanometer resolution. *Science* **313**, 1642–1645 (2006).
[16] Hess, S. T., Girirajan, T. P., & Mason, M. D. Ultra-high resolution imaging by fluorescence photoactivation localization microscopy. *Biophys. J.* **91**, 4258–4272 (2006).
[17] Sakamoto, T., Amitani, I., Yokota, E. & Ando, T. Direct observation of processive movement by individual myosin V molecules. *Biochem. Biophys. Res. Commun.* **272**, 586–590 (2000).
[18] Yamashita, H., Taoka, A., Uchihashi, T., Asano, T., Ando, T. & Fukumori, Y. Single-molecule imaging on living bacterial cell surface by high-speed AFM. *J. Mol. Biol.* **422**, 300–309 (2012).
[19] Ando, T., Kodera, N., Takai, E., Maruyama, D., Saito, K. & Toda, A. A high-speed atomic force microscope for studying biological macromolecules. *Proc. Natl. Acad. Sci. USA* **98**, 12468–12472 (2001).
[20] Schneider, C. A., Rasband, W. S. & Eliceiri, K. W. NIH Image to ImageJ: 25 years of image analysis. *Nat. Methods* **9**, 671–675 (2012).
[21] Fujii, T., Iwane, A. H., Yanagida, T. & Namba, K. Direct visualization of secondary structures of F-actin by electron cryomicroscopy. *Nature* **467**, 724–728 (2010).
[22] Schmitz, S., Schaap, I. A., Kleinjung, J., Harder, S., Grainger, M., Calder, L., *et al*. Malaria parasite actin polymerization and filament structure. *J. Biol. Chem.* **285**, 36577–36585 (2010).
[23] Narita, A., Usukura, E., Yagi, A., Tateyama, K., Akizuki, S., Kikumoto, M., *et al*. Direct observation of the actin filament by tip-scan atomic force microscopy. *Microscopy (Oxf)* **65**, 370–377 (2016).
[24] Müller, D. J., Schoenenberger, C. A., Büldt, G. & Engel, A. Immuno-atomic force microscopy of purple membrane. *Biophys. J.* **70**, 1796–1802 (1996).
[25] Putman, C. A., de Grooth, B. G., Hansma P. K., van Hulst, N. F. & Greve, J. Immunogold labels: cell-surface markers in

atomic force microscopy. *Ultramicroscopy* **48**, 177–182 (1993).
[26] Li, H. LaBean, T. H. & Kenan, D. J. Single-chain antibodies against DNA aptamers for use as adapter molecules on DNA tile arrays in nanoscale materials organization. *Org. Biomol. Chem.* **4,** 3420–3426 (2006).
[27] Barois, N. & Bakke, O. The adaptor protein AP-4 as a component of the clathrin coat machinery: a morphological study. *Biochem. J.* **385**, 503–510 (2005).
[28] Martin, S., Ramm, G., Lyttle, C. T., Meerloo, T., Stoorvogel, W. & James, D. E. Biogenesis of insulin-responsive GLUT4 vesicles is independent of brefeldin A-sensitive trafficking. *Traffic* **1**, 652–660 (2000).
[29] Behnke, J., Eskelinen, E. L., Saftig, P. & Schröder, B. Two dileucine motifs mediate late endosomal/lysosomal targeting of transmembrane protein 192 (TMEM192) and a C-terminal cysteine residue is responsible for disulfide bond formation in TMEM192 homodimers. *Biochem. J.* **434**, 219–231 (2011).
[30] Ardini, M., Giansanti, F., Di Leandro, L., Pitari, G., Cimini, A., Ottaviano, L., *et al*. Metal-induced self-assembly of peroxiredoxin as a tool for sorting ultrasmall gold nanoparticles into one-dimensional clusters. *Nanoscale*. **6**, 8052–8061 (2014).